Journal of Porphyrins and Phthalocyanines
J. Porphyrins Phthalocyanines 2005; **9**: 305-315

Published at http://www.u-bourgogne.fr/jpp/

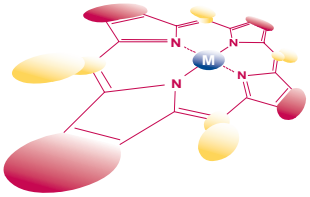

Aza-substitution effect on the Q-band excitations of free-base porphin, chlorin, and bacteriochlorin: SAC-CI theoretical study

Jun-ya Hasegawa[a], Takayuki Kimura[a] and Hiroshi Nakatsuji*[a,b]

[a] *Department of Synthetic Chemistry and Biological Chemistry, Graduate School of Engineering, Kyoto University, Nishikyo-ku, Kyoto 615-8510, Japan*
[b] *Fukui Institute for Fundamental Chemistry, Takano-Nishihiraki-cho 34-4, Sakyo-ku, Kyoto 606-8103, Japan*

Received 1 September 2004
Accepted 20 January 2005

ABSTRACT: Electronic structure of the excited states and absorption spectra of free-base azaporphins, azachlorin, and azabacteriochlorin were systematically investigated by SAC-CI calculations. Aza-substitution at the *meso* position affects the orbital energy of the next-HOMO, and the transition dipole moment enlarges as the number of the substitution increases. Some of the aza-substitutions dramatically affect the direction of the transition dipole, due to reduction of the molecular symmetry, which was studied in detail by a decomposition analysis of the transition dipole moment. Tetraza-substitution in chlorin and bacteriochlorin increases the oscillator strength more than that of tetrazaporphin. The mechanism underlying these changes originates mainly from the relaxation of near-degeneracy in the main configurations. These findings would be useful for the application to the molecular design of the excited states.

KEYWORDS: azaporphin, excited state, SAC-CI, transition dipole moment.

INTRODUCTION

Porphyrins and the related cyclic-tetrapyrroles have attracted interest for a long time as key compounds in biology, chemistry, and material science [1-3]. One of the most important properties of these compounds is their absorption bands in the UV-vis regions: Q- and B- (Soret) bands. In green plants and photosynthetic bacteria, the Q-band absorptions of chlorophylls and bacteriochlorophylls work for light-harvesting [4, 5]. Phthalocyanines have enhanced Q-band absorption and their optical property are very useful not only for industrial pigments but for functional materials [3, 6, 7]. Recently, metal-porphyrins were used for constructing a dendritic system [8]. In medical science, porphyrins are used as the photosensitizer for photodynamic therapy (PDT) [9] and the photochemistry starting with the Q-band excitation is used for treatment of cancer [9]. Therefore, it is very important to understand the character of the low-lying excited states. This basic understanding would be useful for designing excited states of porphyrin compounds, namely for controlling the transition energy and intensity of the absorption bands especially in the visible region (Q-bands). For the PDT case, one of the desired property to be a useful photosensitizer is that it should have a significant absorption in the long wavelength region (700-800 nm) [9].

There are several strategies to realize the strong absorption in the visible region [1, 2]. Aza-substitution at the *meso*-position of the porphyrin leads tetrazaporphin (**TAP**) and phthalocyanine (**Pc**) [6] to have the Q-band absorption at much larger wavelengths than their parent compound, porphin (**P**). Extension of the π-conjugation in **Pc** successfully enhances Q-band intensity [10]. In

*Correspondence to: Hiroshi Nakatsuji, email: hiroshi@sbchem.kyoto-u.ac.jp

Published on web 07/12/2005

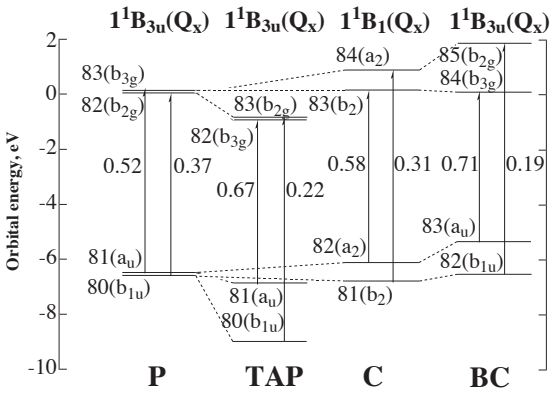

Fig. 1. Energy levels of Gouterman's four-orbitals of **P**, **TAP**, **C**, and **BC**. The main configurations (indicated by the arrays) of the lowest excited states (Q_x) are also shown. The values beside the arrays are the weight of the main configuration obtained by the SAC-CI calculations

contrast, introducing the reduced-pyrrole units also leads to stronger absorption as seen in chlorin (**C**) and bacteriochlorin (**BC**). Alternating the position of pyrroles and methine units also enhances absorption intensity as seen in porphycenes (**Pcene**) [11] and hemiporphycene (**hPcene**) [12].

To figure out how to control the Q-band absorption, it would be necessary to understand the mechanism of the Q-band changes observed in several basic porphyrin compounds. Figure 1 shows the energy levels of Gouterman's four-orbitals [13] of free-base porphin (**P**), free-base tetrazaporphin (**TAP**), free-base chlorine (**C**) and free-base bacteriochlorin (**BC**). The main configurations and their weight for the Q_x band are also shown. The orbital shapes of the four-orbitals of **P** are shown in Fig. 2 as a typical example.

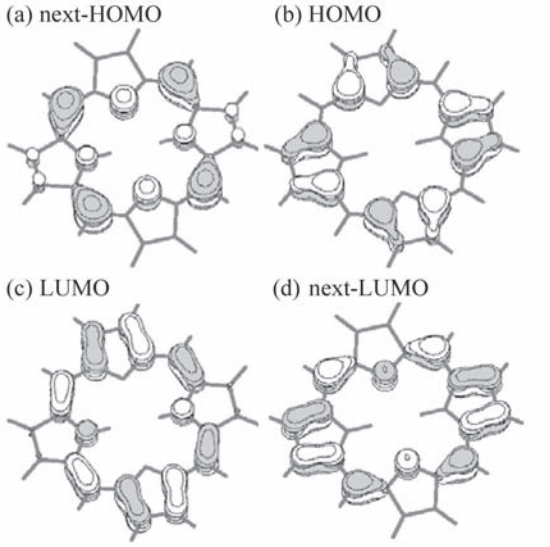

Fig. 2. Four orbitals of free-base porphin (**P**). (a) Next-HOMO, (b) HOMO, (c) LUMO, and (d) next-LUMO

The most basic compound, **P**, has very small Q-band absorption. The energy levels of HOMO (MO 81) and next-HOMO (MO 80) are very close to each other. The same is seen in those of LUMO (MO 82) and next-LUMO (MO 83). As a consequence, the two excitations, 81 → 83 and 80 → 82, have similar weight in the wave function. Since these two configurations have a similar amount of transition dipole moment with a different sign, the total transition dipole of the states becomes very small due to the mutual cancellation [14]. It is well-known that tetra-aza substitution at the *meso*-position (**TAP**, see Fig. 3 (g)) significantly increases the Q-band intensity [15, 16]. As shown in Fig. 2, since the next-HOMO of **P** has a large amplitude at the *meso*-position, tetraza-

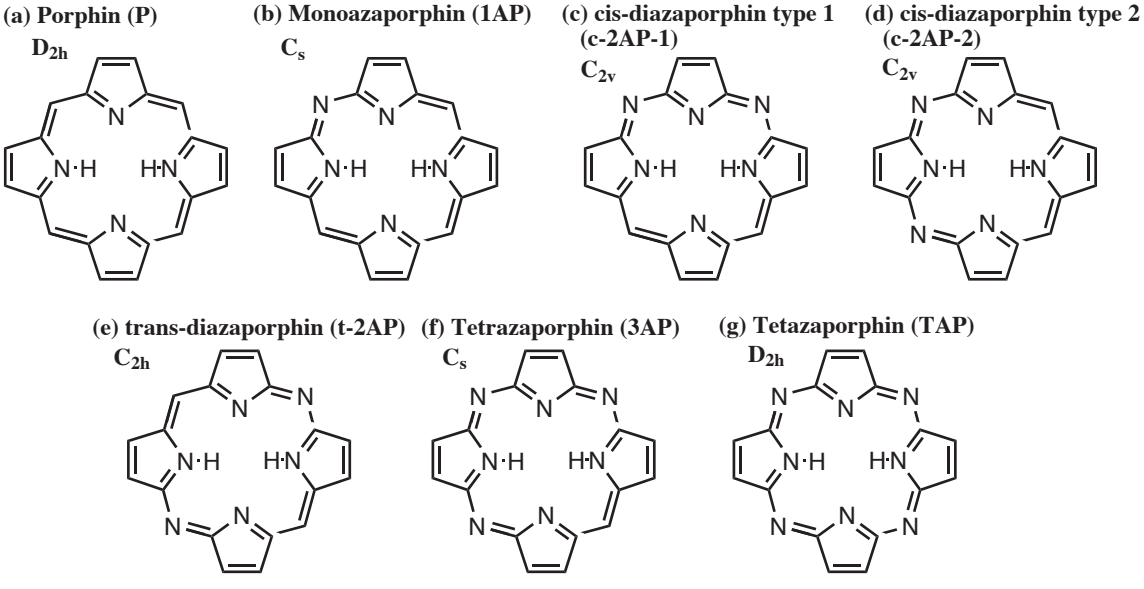

Fig. 3. Structure and symmetry of free-base azaporphins

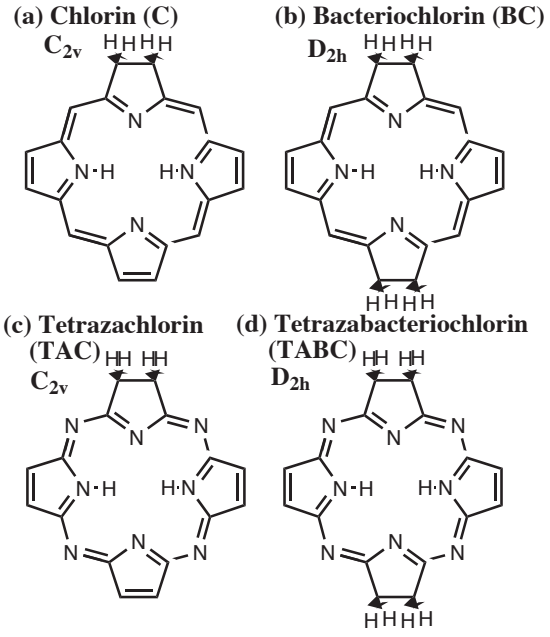

Fig. 4. Structure and symmetry of free-base chlorins and bacteriochlorins

substitutions stabilizes the energy level of the next-HOMO much more than that of other three orbitals. This stabilization relaxes the near-degeneracy of the two configurations, and cancellation of the transition moment becomes incomplete [14].

As seen in green plants, **C** (Fig. 4a) and **BC** (Fig. 4b) also have large Q-band absorptions. These compounds have reduced-pyrrole rings: saturated carbon atoms in the pyrrole units. This modification shrinks the size of the π-conjugation in the HOMO and LUMO in Fig. 2, and their orbital energies are unstabilized. The near-degeneracy of the two configurations is also relaxed in these cases, and the residual transition moment contributes to the absorption intensity [17]. Therefore, a principle for tuning the Q_x-band absorption is to control the near-degeneracy of the main configurations, which causes an incomplete cancellation of the transition dipole moment.

Among the porphyrins mentioned above, aza-substitution would be one of the promising approaches for controlling the Q-band. A systematic study on the effect of aza-substitutions would be useful for a basic understanding and practical applications. Furthermore, a combination of the strategies has a possibility to lead to a fruitful result as the case of **Pc**. The reduced-pyrrole unit in **C** and **BC** unstabilizes the HOMO and next-LUMO level [17], while tetraza-substitution in **TAP** stabilizes the next-HOMO [14]. These two substitutions affect the different orbitals in a specific way. It is therefore interesting to examine the combining effect of tetraza-substitution and introduction of the reduced pyrrole units. Thus, tetrazachlroin (**TAC**, Fig. 4c) and tetrazabacteriochlorin (**TABC**, Fig. 4d) were designed and their excited states and Q-bands are investigated in the present study. Actually, we have found in the literature [16] that these compounds have already synthesized [18-20] and the electronic excitation spectrum was also published [16, 20, 21].

For designing a pigment having desired excited-state properties, the basic understanding and the predictions must be based on accurate calculations by using a reliable method. We use here Symmetry-Adapted Cluster (SAC) [22]-Configuration Interaction (CI) [23-25] method [26]. The SAC-CI method has been established as an accurate excited-state method and already applied to many systems from atoms to bio-molecules [26]. The SAC-CI theory is equivalent to Coupled-Cluster Linear Response Theory (CCLRT) [27-31] and Equation Of Motion-Coupled Cluster theory (EOM-CC) [32, 33]. A previous study showed that these methods gave the same numerical results [34]. The SAC-CI method has been applied to the excited states of many porphyrins and related compounds [14, 17, 26, 35], and the SAC-CI theoretical spectrum is very useful for assigning observed absorption spectra.

In this paper, we describe a theoretical study on the low-lying excited state, Q-bands, of aza-substituted porphin, chlorin, and bacteriochlorin. To our knowledge some of the compounds have not yet synthesized. In section 3, we first examine the effect of aza-substitutions at the *meso* position in a series of azaporphyrins. The electronic structures and the transition properties are discussed. In section 4, **TAP** is adopted for a starting building block and the combination effect, namely tetra-aza-substitution and reduction of pyrrole rings, is examined in **TAC** and **TABC**. The results of the calculations are compared with experimental results so far reported.

COMPUTATIONAL DETAILS

Details about the SAC-CI method can be found in previous articles and reviews [26, 34]. In this section, we describe only the details of the calculations.

Geometry optimization was carried out by using Density Functional Theory (DFT) [36-38] calculation with B3LYP [39, 40] functional. The basis sets employed are valence-double-ζ plus polarization (VDZP) quality. The 6-31g(d) [41, 42] and 4-31g [43] sets were used for C and N atoms and for H atom, respectively. Molecular symmetry to which the optimized geometry belongs is summarized in Fig. 3 and 4 with their molecular structures.

Single-point SAC-CI calculations were performed using the optimized geometries. The basis sets used are of double-ζ quality. Huzinaga's (63/5)/[5121/41] sets

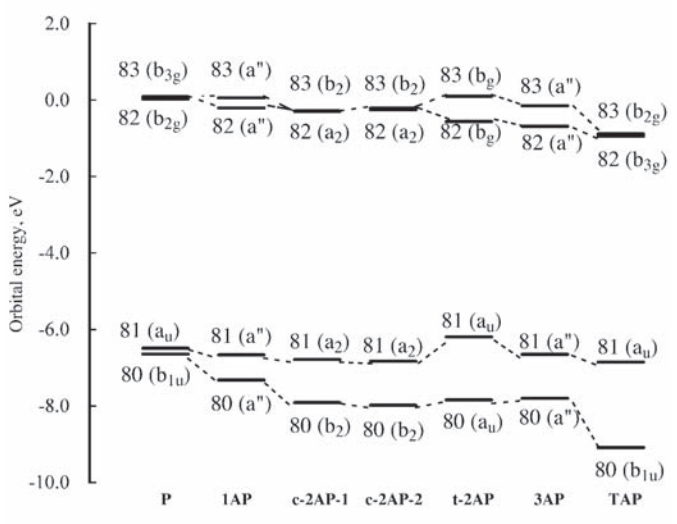

Fig. 5. Comparison of the energy levels of the four-orbitals in free-base azaporphins

[44] were adopted for C and N atoms, and Huzinaga's (4)/[31] set [45] were for H atoms. In our experience, polarization functions gave only minor corrections to the excited states of porphyrin compounds [46]. The active space includes all the valence orbitals. The 1s orbitals and their corresponding virtual orbitals were treated as frozen orbitals. All single-excitation and selected double-excitation operators were included in the SAC/SAC-CI wave functions. The perturbation-selection method [47] was used for selecting doubles. The CI-singles wave functions were used for the reference states in the perturbation selection. The energy threshold for the ground and excited states are 1×10^{-5} and 1×10^{-6} au, respectively.

All calculations used the gaussian03 program system [48] in which the SAC-CI program has been implemented and released.

RESULTS AND DISCUSSION

Systematic investigation on the aza-substitutions at *meso*-position of free-base porphin

In this section, the low-lying excited states of aza-porphins are described. The compounds investigated are from mono- to tetra-aza-substituted free-base compounds which are shown in Fig. 3. For the diaza-compounds, there is one trans isomer (**t-2AP**) and two cis-isomers (**c-2AP-1** and **c-2AP-2**).

Figure 5 shows the energy levels of the four-orbitals. It is clearly seen that the next-HOMO level is affected by the aza-substitution at the *meso*-position. This stabilization enlarges almost in proportional to the number of the introduced nitrogen atoms. Tetra-aza substitution, **TAP**, has the largest stabilization in the series of azaporphins. The nitrogen atom has a 2p level that is lower than that of the carbon atom. Regarding unoccupied MOs, there are only minor changes in the orbital energy levels. One exception is the energy splitting between the LUMO and next-LUMO levels of **t-2AP** and **3AP**. A possible reason is symmetry-lowering due to the asymmetric aza-substitutions. In Fig. 6, the four-orbitals of **t-2AP** and **3AP** are shown. In the LUMO of **t-2AP**, there is amplitude on all the nitrogen atoms in the *meso* position. In contrast, in the next-LUMO, there is a node on the nitrogen atoms. Similarly in **3AP**, although the LUMO has an amplitude on all of the nitrogens, the next-LUMO has less orbital population and there is a node passing through a nitrogen atom. In addition, these LUMO and next-LUMO belong to the same irreducible representation: b_g in **t-2AP**

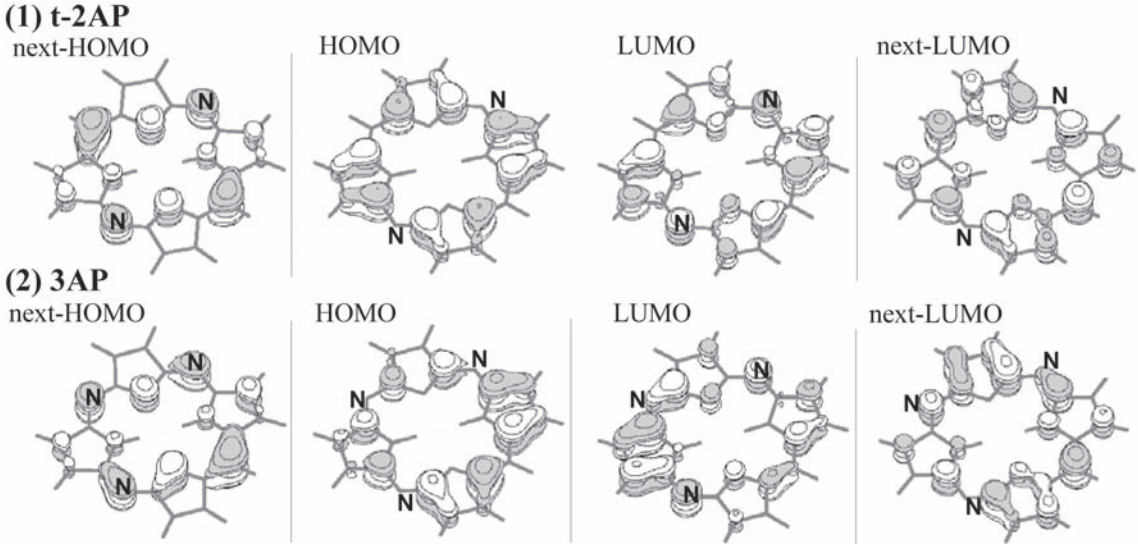

Fig. 6. Four-orbitals of (1) trans-diazaporphin (**t-2AP**) and (2) tetrazaporphin (**3AP**)

Table 1. Excited states of free-base azaporphins calculated by the SAC-CI method

State	SAC-CI			Exptl.
	Main configurations	Excitation energy, eV	Oscillator strength, au	Excitation energy, eV
P (porphin)				
1^1B_{3u}	0.71 (80 → 82) + 0.62 (81 → 83)	1.88	0.0×10^{-3}	1.98,[a] 2.03[b]
1^1B_{2u}	0.69 (80 → 83) - 0.67 (81 → 82)	2.34	1.3×10^{-3}	2.42,[a] 2.39[b]
1AP (monoazaporphin)				
$2^1A'$	-0.60 (81 → 82) + 0.46 (80 → 83) - 0.23 (80 → 82) - 0.19 (81 → 83)	1.90	0.0368	2.03[b]
$3^1A'$	0.47 (80 → 82) + 0.48 (81 → 83) - 0.46 (81 → 82) + 0.27 (80 → 83)	2.39	0.0428	2.32[b]
c-2AP-1 (cis-diazaporphin type 1)				
1^1B_1	0.73 (81 → 83) - 0.59 (80 → 82)	1.80	0.0457	
2^1A_1	-0.68 (81 → 82) - 0.43 (80 → 83)	1.84	0.0563	
c-2AP-2 (cis-diazaporphin type 2)				
2^1A_1	-0.79 (81 → 82) - 0.49 (80 → 83)	2.02	0.0970	
1^1B_1	-0.83 (81 → 83) + 0.47 (80 → 82)	2.39	0.1375	
t-2AP (trans-diazaporphin)				
1^1B_u	-0.56 (81 → 82) - 0.47 (81 → 83) - 0.46 (80 → 82) + 0.38 (80 → 83)	1.73	0.0573	2.00[b]
2^1B_u	0.50 (81 → 83) + 0.58 (81 → 82) - 0.47 (80 → 82) - 0.33 (80 → 83)	2.18	0.0879	2.28[b]
3AP (triazaporphin)				
$2^1A'$	0.67 (81 → 82) - 0.32 (80 → 83) + 0.21(81 → 83) + 0.15 (80 → 82)	1.68	0.1117	
$3^1A'$	0.67 (81 → 83) + 0.42 (80 → 82) - 0.08 (80 → 83) + 0.04(81 → 82)	1.98	0.0771	
TAP (tetrazaporphin)				
1^1B_{3u}	0.82 (81 → 82) + 0.47 (80 → 83)	2.05	0.2000	2.01[c]
1^1B_{2u}	-0.85 (81 → 83) + 0.44 (80 → 82)	2.40	0.2239	2.27[c]

[a] In vapor phase [50]. [b] In $CHCl_3$ [49]. [c] In chlorobenzene [15].

(C_{2h}) and a" in **3AP** (C_s). Therefore, the interaction between the LUMO and the next-LUMO causes the energy splitting.

In Table 1, the low-lying excited states of the free-base azaporphins are summarized. For **P**, **1AP**, **t-2AP**, and **TAP**, the experimental excitation energy observed in $CHCl_3$ is available for comparison, although most of them are spectra in solution. Table 1 shows reasonable agreement with the experimental data. The RMS deviation is around 0.12 eV, and the maximum error is 0.27 eV in the 1^1B_u state of **t-2AP**. In Fig. 7, the SAC-CI theoretical spectra for **P**, **1AP**, **t-2AP**, and **TAP** are compared with the experimental spectra observed in $CHCl_3$ [49]. The theoretical result reproduced the spectral features in the relative peak position and in the relative ordering of the absorption strength among the four aza-porphins.

The main configurations of the first and second excited states are composed of excitations within the four-orbitals. Therefore, the transition moment and oscillator strength are determined by configuration mixing within the four-orbital excitations. For **P**, the main configurations of the 1^1B_{3u} and 1^1B_{2u} states are near-degenerate, and the oscillator strength becomes very small due to cancellation of the transition moment between the two main configurations [14]. This is clearly illustrated in Table 2. In the first excited state (1^1B_{3u}), the contribution to transition moment from the excitations, 80 → 82 and 81 → 83, are 3.09 and -2.99, respectively. Total amount of transition moment

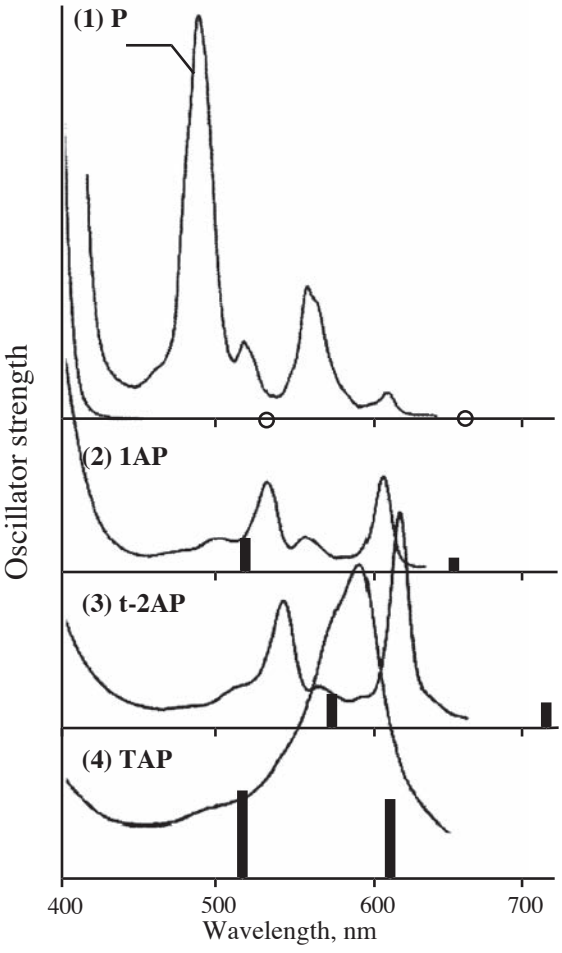

Fig. 7. Absorption spectra in $CHCl_3$ and SAC-CI theoretical spectra of (1) porphin (**P**), (2) monoazaporphin (**1AP**), (3) trans-diazaporphin (**t-2AP**), and (4) tetrazaporphin (**TAP**)

becomes very small. Similarly, in the second excited state (1^1B_{2u}), the contributions from 80 → 83 (-2.88) and 81 → 82 (3.06) cancel each other. However, aza-substitutions relax such degeneracy, because the next-HOMO is stabilized. The effects clearly appear in the magnitude of the oscillator strength. The 1^1B_{3u} and 1^1B_{2u} states of **TAP** have the largest oscillator strength of all the azaporphins, which is around 10^3 times larger than that of **P**. As seen in Table 2, the decomposition analysis shows that the difference in the orbital transition dipole also contributes to the enhancement of the net moment. For instance, < 80 | r | 82 > and < 81 | r | 83 > in **P** are 3.07 and -3.39 au, respectively, whose absolute values are close each other. The corresponding entities in **TAP** are 2.59 and -3.58 au, respectively.

The direction of the transition dipole moment is an important factor for designing photochemical systems, especially if the excitation energy transfer (EET) is involved. The direction of the moment determines the magnitude of the interaction between the excited states. Figure 8 shows the direction of the moment for the first and second excited states. The length of the arrows represents the vector length of transition moment. It is clearly indicated that the transition moments increase almost in proportional to the number of aza-substitutions. One interesting point is that the angle of the transition moment is different from the ordinary axis in **1AP**, **t-2AP**, and **3-AP**. In **1AP** and **t-2AP**, the angle between the first and second excited states is far from 90 degrees. The reason is in molecular symmetry. In **P**, **c-2AP-1**, **c-2AP-2**, and **TAP**, the direction of the transition moment is determined by the irreducible representation (IREP) to which the excitation belongs. The angle between the two states are thus orthogonal each other. For

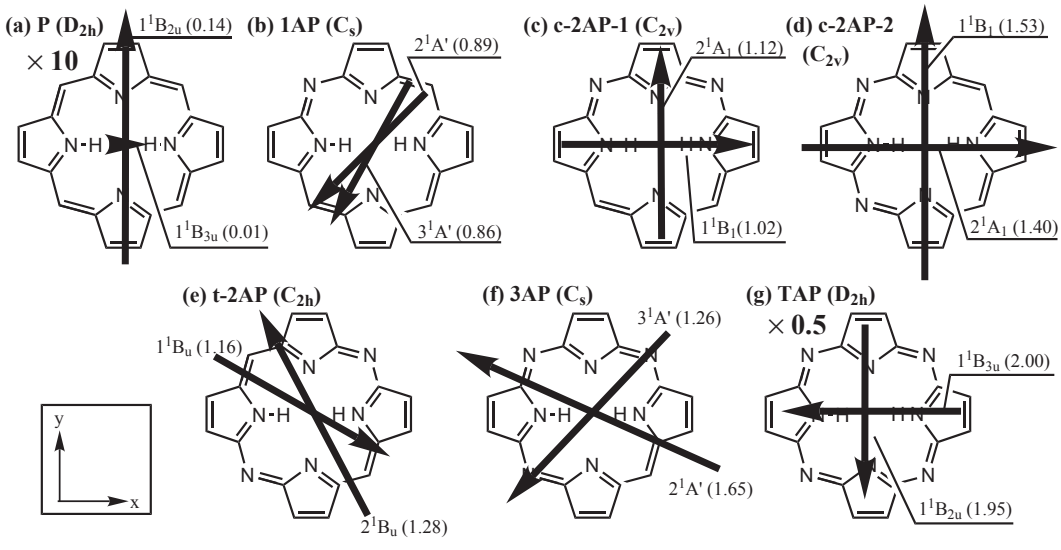

Fig. 8. Transition dipole moment of free-base azaporphins. The number in the parenthesis denotes length of transition dipole. For **P** and **TAP**, the length of the arrow is scaled by 10 and 0.5, respectively

Table 2. Decomposition analysis for the transition dipole moment of several aza-porphins calculated by the SAC-CI method

	Orbital TDM [a]		Q_1 (first excited state)			Q_2 (second excited state)		
	$< i \mid r \mid a >$ [b]		C_{ia} [c]	$< HF \mid r \mid i \rightarrow a > C_{ia}$		C_{ia}	$< HF \mid r \mid i \rightarrow a > C_{ia}$	
	x [d]	y [d]		x	y		x	y
P								
80 → 82 (b_{3u})	3.07	-	0.71	3.09	-	-	-	-
81 → 83 (b_{3u})	-3.39	-	0.62	-2.99	-	-	-	-
80 → 83 (b_{2u})	-	-2.94	-	-	-	0.69	-	-2.88
81 → 82 (b_{2u})	-	-3.24	-	-	-	-0.67	-	3.06
Σ(4-orb. ex.) [e]				0.09				0.19
$< SAC \mid r \mid SAC\text{-}CI >$ [f]				0.01				0.15
1AP								
80 → 82	-2.24	1.84	-0.23	0.72	-0.59	0.47	-1.50	1.23
81 → 83	2.51	-2.06	-0.19	-0.69	0.56	0.48	1.70	-1.40
80 → 83	1.79	2.03	0.46	1.16	1.31	0.27	0.69	0.78
81 → 82	2.20	2.45	-0.60	-1.88	-2.09	-0.46	-1.43	-1.59
Σ(4-orb. ex.)				-0.69	-0.81		-0.53	-0.97
$< SAC \mid r \mid SAC\text{-}CI >$				-0.63	-0.63		-0.40	-0.75
t-2AP								
80 → 82	2.02	2.07	-0.46	-1.31	-1.34	-0.47	-1.33	-1.37
81 → 83	-2.32	-2.37	-0.47	1.53	1.56	-0.50	1.64	1.67
80 → 83	-1.98	1.77	0.38	-1.07	0.95	-0.33	0.92	-0.82
81 → 82	2.61	2.33	-0.56	2.07	-1.85	0.58	-2.14	1.91
Σ(4-orb. ex.)				1.22	-0.67		-0.92	1.39
$< SAC \mid r \mid SAC\text{-}CI >$				1.03	-0.54		-0.69	1.08
3AP								
80 → 82	1.74	1.79	0.15	0.38	0.39	0.41	1.02	1.05
81 → 83	-2.24	-2.32	0.21	-0.68	-0.70	0.67	-2.11	-2.18
80 → 83	-1.93	1.67	-0.32	0.88	-0.76	-0.08	0.23	-0.20
81 → 82	-2.50	2.21	0.66	-2.36	2.08	0.04	-0.17	0.15
Σ(4-orb. ex.)				-1.78	1.01		-1.03	-1.18
$< SAC \mid r \mid SAC\text{-}CI >$				-1.44	0.80		-0.89	-0.90
TAP								
80 → 82 (b_{2u})	-	2.42	-	-	-	0.44	-	1.52
81 → 83 (b_{2u})	-	3.39	-	-	-	-0.84	-	-4.06
80 → 83 (b_{3u})	2.59	-	0.47	1.72	-	-	-	-
81 → 82 (b_{3u})	-3.58	-	0.82	-4.18	-	-	-	-
Σ(4-orb. ex.)				-2.46				-2.53
$< SAC \mid r \mid SAC\text{-}CI >$				-2.00				-1.95

[a] Transition dipole moment in atomic unit. [b] "i" and "a" denote the orbital indices included in the excited configurations. For instance, (i,a) = (80,82) if the corresponding configuration is 80 → 82. [c] SAC-CI coefficient for the configuration I → a. [d] The x- and y-axes are indicated in Fig. 8. [e] Summation over the contributions from the four-orbital excitations. [f] Transition dipole moment calculated with the SAC (ground-state) and SAC-CI (excited-state) wave functions.

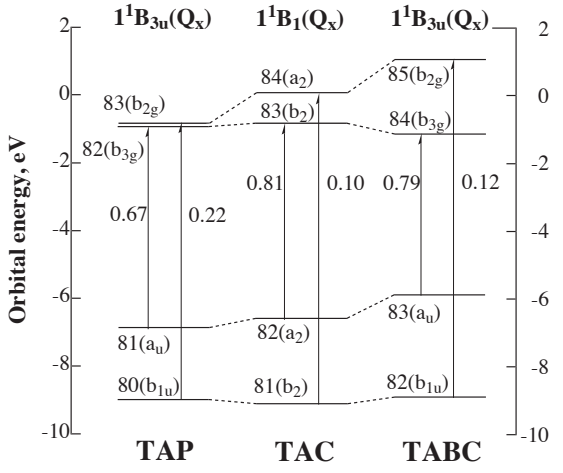

Fig. 9. Gouterman's four-orbital levels of **TAP**, **TAC**, and **TABC**. The main configurations (indicated by arrays) of the lowest excited states (Q_x) are also shown. The values beside the arrays are the weight of the main configuration obtained by the SAC-CI calculations

instance in **P**, the excitations 80 → 82 and 81 → 83 belong to b_{3u} symmetry (x-direction), while the excitations 80 → 83 and 81 → 82 to b_{2u} symmetry (y-direction). However, in **1AP**, **t-2AP**, and **3-AP**, all four-orbital excitations are in the same IREP, and the configuration mixing among the excitations can give the exotic direction of the transition moment. As shown in Table 1, **1AP**, **t-2AP**, and **3-AP** have all the four-orbital excitations in the wave functions.

To analyze these effects in details, we carried out a decomposition analysis for the transition dipole moment. In Table 2, the results of the analysis for **1AP**, **t-2AP**, and **3-AP** are shown, together with the data for **P** and **TAP**. The x- and y-axes are placed on the molecular plane, and the x-direction is taken as N(-H)-N(-H) axis. These definitions are indicated in Fig. 8. The reason why the direction of the moment is far from the x- or y-axis is in the direction of the orbital transition dipole, $< i \mid r \mid a >$. In **P** and **TAP**, this entity is strictly related to the symmetry. The excitations belonging to the b_{3u}/b_{2u} symmetry has the directions parallel to the x-/y-axis, respectively. However, in **1AP**, **t-2AP**, and **3-AP**, this symmetry property is lost already in the orbital transition dipole moment, $< i \mid r \mid a >$, even though the orbital characters still resemble those of **P**, as seen from the orbital shapes in Figs 2 and 6.

The reason for the small angles between the first and second excited states, especially seen in **1AP** and **t-2AP**, is a result of the configuration interactions. In these compounds, the two excitations 80 → 82 and 81 → 83 cancel their transition moment each other as in the Q-bands of **P**, while the cancellation in the 80 → 83 and 81 → 82 case is incomplete as in the Q-bands of **TAP**. Since the excitations 80 → 83 and 81 → 82 are included in the main configurations of the first and second excited states, the direction of the transition dipole reflects that of these two excitations. The contributions from the 80 → 82 and 81 → 83 are anyway minor, even though these two excitations become dominant configurations. For example in the first excited state of **1AP**, the contributions from 80 → 82 and 81 → 83 are 0.72 and -0.69 in the x-direction and -0.59 and 0.56 in the y-direction, respectively, as shown in Table 2. The sum of the contributions becomes only 0.03 (x-direction) and -0.03 (y-direction), respectively: the same situation in the Q bands of **P**. On the other hand, the excitations 80 → 83 and 81 → 82 remarkably contribute to the net transition dipole, because of incomplete cancellation of the moment as seen in the Q-bands of **TAP**: -0.72 in the x-direction and -0.78 in the y-direction. The same is seen in the other states of **1AP** and **t-2AP**. It is interesting that only a few substitutions can lead to such a large difference in the transition moment, and these findings might be applicable to the design of photochemical systems, especially for energy transfer systems.

Tetraza-substitution in chlorin and bacteriochlorin units

Chlorin (**C**) and bacteriochlorin (**BC**) have Q-band absorptions larger than those of porphin (**P**). On the other hand, tetraza-substitution to **P**, that gives **TAP**, also increases the Q-band absorption intensity. In this section, a combination of these two strategies is examined: excited states of tetrazachlorin (**TAC**) and tetrazabacteriochlorin (**TABC**) are analyzed by the SAC-CI method.

In Fig. 9, the energy levels of the four-orbitals are shown. Compared to **TAP**, the HOMO and next-LUMO levels of **TAC** and **TABC** shift to a higher-energy region, due to introduction of the reduced-pyrrole rings in the **C** and **BC** units. As a consequence, the HOMO-LUMO gaps of **TAC** and **TABC** remarkably decrease, while those between the next-HOMO and the next-LUMO increase. Based on these changes in the orbital energy levels, we can simply expect that the near-degeneracy of the two configurations in the Q_x band would be further relaxed and the Q_x state would show a red-shift and increase the transition moment.

In Table 3, we list the excited states of **TAC** and **TABC**, together with those of **P**, **C**, **BC**, and **TAP**. The SAC-CI excitation energy is compared with experimental values observed for similar compounds, **TAC** and **TABC** having dibenzobarreleno groups. The average error is 0.15 eV. Figure 10 compares the SAC-CI results with the experimental absorption spectra for **TAC** and **TABC** having dibenzobarreleno groups [16, 19]. The theoretical result reproduced the spectral changes among these compounds: the

Table 3. Excited states of free-base P, C, BC, TAP, TAC, and TABC

State	SAC-CI				Exptl.
	Main configuration (C > 0.2)	Excitation energy, eV	Transition dipole, au	Oscillator strength, au	Excitation energy, eV
porphin (**P**)					
1^1B_{3u}	0.71 (80 → 82) + 0.62 (81 → 83)	1.88	0.0066	0.6×10^{-3}	1.98,[a] 2.03[b]
1^1B_{2u}	0.69 (80 → 83) - 0.67 (81 → 82)	2.34	0.1482	0.0×10^{-3}	2.42,[a] 2.39[b]
chlorin (**C**)					
1^1B_1	0.76 (82 → 83) - 0.56 (81 → 84)	1.64	1.1445	0.0526	1.98[c]
2^1A_1	0.67 (81 → 83) + 0.60 (82 → 84)	2.06	0.1226	0.0008	2.29[c]
bacteriochlorin (**BC**)					
1^1B_{3u}	0.84 (83 → 84) - 0.44 (82 → 85)	1.44	2.3494	0.1953	(1.6)[d]
1^1B_{2u}	0.80 (82 → 84) - 0.52 (83 → 85)	2.43	1.0990	0.0719	(2.3)[d]
tetrazaporphin (**TAP**)					
1^1B_{3u}	0.82 (81 → 82) + 0.47 (80 → 83)	2.05	1.9968	0.2000	2.01[e], 1.99[f].
1^1B_{2u}	-0.85 (81 → 83) + 0.44 (80 → 82)	2.40	1.9535	0.2239	2.27[e], 2.24[f]
tetrazachlorin (**TAC**)					
1^1B_1	0.90 (82 → 83) + 0.31 (81 → 84)	1.66	2.6651	0.2888	1.83[g]
2^1A_1	-0.85 (82 → 84) - 0.36 (81 → 83)	2.17	1.8225	0.1764	2.34[g]
tetrazabacteriochlorin (**TABC**)					
1^1B_{3u}	0.89 (83 → 84) + 0.34 (82 → 85)	1.46	3.1533	0.3568	1.57[g]
1^1B_{2u}	0.74 (83 → 85) - 0.59 (82 → 84)	2.76	0.6767	0.0310	2.68[g]

[a] In vapor phase [50]. [b] In $CHCl_3$ [49]. [c] In benzene [51]. [d] Data for bacteriopheophrorbide [52]. [e] In chlorobenzene [15]. [f] In $CHCl_3$ [21] [g] TAC and TABC with dibenzobarreleno group [21].

order of the excitation energy for the first and second excited states is **TAP** > **TAC** > **TABC** (red-shift) and **TAP** < **TAC** < **TABC** (blue-shift), respectively. The intensity of the second excited states is **TAP** > **TAC** > **TABC**.

In **TAC** and **TABC**, the orbital energy level of the HOMO becomes unstable due to the reduction in the pyrrole rings. As clearly seen in Fig. 9, HOMO-LUMO gap then decreases in **TAC** and **TABC**, which causes the red-shift of the first excited states. The main configuration of the second excited states is the excitation from the HOMO to the next-LUMO. As seen in Fig. 9, the energy gap between the HOMO and the next-LUMO increases in **TAC** and **TABC**, which causes the blue-shift of the second excited state. The intensity decrease in the second excited states of **TAC** and **TABC** would be related to the near-degeneracy in the main configurations. As seen in Table 3, the main configurations of the second excited states are the excitations from the HOMO to the next-LUMO and from the next-HOMO to the LUMO. Near-degeneracy in these two configurations increases in **TAC** and **TABC**. As seen in Fig. 9, the energy gaps between the HOMO to the next-LUMO and between the next-HOMO to the LUMO become closer, when the pyrrole rings are reduced. The next-LUMO levels are affected more than the HOMO levels.

With respect to the intensity of the first peak, **TAP**, **TAC**, and **TABC** have a similar absorbance in the experimental spectra [16, 19] shown in Fig. 10. However, the order of the intensity among the three compounds differs from those observed in hexane [20] and in chloroform [21]. In our theoretical result in the vapor-phase, the oscillator strengths of the first excited state of **TAC** and **TABC** are calculated to be 0.2888 and 0.3568 au, respectively. These values are larger than that of **TAP** (0.2000 au), and they are 1000 times larger than that of **P**. As mentioned in the previous section, this increase is relevant to the relaxation of near-degeneracy in the two main configurations. The ratio of the coefficient between HOMO → LUMO and next-HOMO → next-LUMO configurations is around 8.1 : 1.0 in **TAC** and 6.6 : 1.0

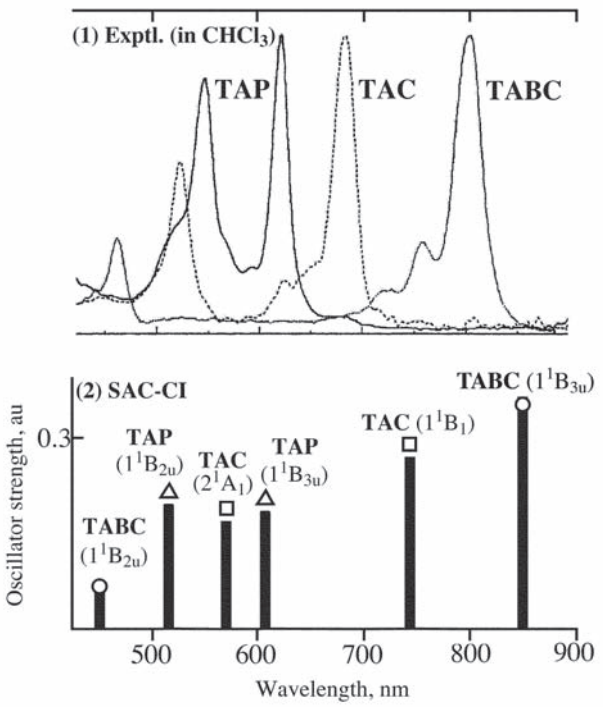

Fig. 10. Electronic excitation spectra of free-base tetrazaporphin (TAP), tetrazachlorin (TAC), and tetraza-bacteriochlorin (TABC). (1) Experimental spectra in $CHCl_3$ [16]. (2) SAC-CI theoretical spectra. The symbols, open-triangles, open-squares, and open-circles, indicate TAP, TAC, and TABC, respectively

in **TABC**, while 3.0 : 1.0 in **TAP**, as shown in Fig. 9. The transition moment of the 1^1B_{3u} state of **TABC** (0.3568 au) is larger than that of the 1^1B_1 state of **TAC** (0.2888 au), although the relaxation effect of **TAC** is larger than that of **TABC**. The reason could be the increase of the transition moment of the HOMO → LUMO configuration by tetraza-substitutions, as in the case of free-base porphin.

CONCLUSION

In this communication, we report a systematic study on the excited states and absorption spectra of free-base azaporphins, azachlorin, and azabacteriochlorin. The SAC-CI calculations were performed for the six azaporphins from mono- to tetra-aza-substitutions. The aza-substitution at the *meso* positions affects the next-HOMO level and the transition dipole moment of the first excited state enlarges as the number of the substitution increases. In monoazaporphin (**1AP**), trans-diazaporphin (**t-2AP**), and triazaporhin (**3AP**), the aza-substitutions reduce the molecular symmetry and all four-orbital excited configurations are able to mix with each other. As a consequence, the direction of the transition moment shows remarkable changes. These would be interesting examples that could be applicable to designing excitation-energy transfer systems.

Two strategies for modifying the excited state of porphyrins are combined and examined: tetraza-substitution in chlorin and bacteriochlorin. The SAC-CI results are in reasonable agreement to the experimental spectra. In the first excited state of **TAC** and **TABC**, the SAC-CI results show that introduction of the reduced-pyrroles shifts the excitation energy to lower-energy region and increases the oscillator strength more than **TAP**. The reason of these changes originates mainly from the shift of the HOMO and next-LUMO levels which causes relaxation of the near-degeneracy in the main configuration. **TAP**, **TAC**, and **TABC** have a strong oscillator strength in different visible regions. Therefore, these basic building units are useful for the excited-states molecular design.

Acknowledgements

This study was supported by a Grant-in-Aid for Creative Scientific Research from the Ministry of Education, Culture, Sports, Science and Technology of Japan and also in part by the Matsuo Foundation.

REFERENCES

1. Dolphin D, Ed. *The Porphyrins*; Academic Press: New York, 1978.
2. Kadish KM, Smith KM and Guilard R, Eds. *The Porphyrin Handbook*; Academic Press: New York, 2000.
3. Kadish KM, Smith KM and Guilard R, Eds. *The Porphyrin Handbook II*; Academic Press: New York, 2003; Vol. 15-20.
4. Sundstroem V, Pullerits T and Grondelle Rv. *J. Phys. Chem. B* 1999; **103**: 2327.
5. Schulten K. In *Simplicity and Complexity in Proteins and Nucleic Acids*, Frauenfelder H, Deisenhofer J, Wolynes PG. (Eds.) Dahlem University Press: Berlin, 1999; pp 227-253.
6. Moser FH and Thomas AL. *The Phthalocyanines*; CRC Press: Boca Raton, 1983
7. Leznoff CC and Lever ABP. *Phthalocyanines - Properties and Applications*; VCH Publishers: New York, 1993
8. Choi M-S, Aida T, Yamazaki T and Yamazaki I. *Angew. Chem. Int. Ed.* 2001; **40**: 3194.
9. Pandey RK and Zheng G. In *The porphyrin handbook, vol. 6*, Vol. 6, Kadish KM, Smith KM, Guilard R. (Eds.) Academic press: New York, 2000; pp 157-230.
10. Edwards L and Gouterman M. *J. Mol. Spectrosc.* 1970; **33**: 292.
11. Vogel E, Kocher M, Schmickler H and Lex J. *Angew. Chem. Int. Ed. Engl.* 1986; **25**: 257.
12. Sessler JL, Brucker EA, Weghorn SJ, Kisters M, Schafer M, Lax J and Vogel E. *Angew. Chem.*

1994; **106**: 2402.
13. Gouterman M. *J. Mol. Spectrosc*. 1961; **6**: 138.
14. Toyota K, Hasegawa J and Nakatsuji H. *Chem. Phys. Letters* 1996; **250**: 437-442.
15. Linstead RP and Whally M. *J. Chem. Soc*. 1952: 4839.
16. Kobayashi N. In *The Porphyrin Handbook, Vol. 2*, Vol. Vol. 2, Kadish KM, Smith KM, Guilard R. (Eds.) Academic Press: New York, 2000; pp 301-360.
17. Hasegawa J, Ozeki Y, Ohkawa K, Hada M and Nakatsuji H. *J. Phys. Chem. B* 1998; **102**: 1320-1326.
18. Ficken GE, Linstead RP, Stephen E and Whalley M. *J. Chem. Soc*. 1958: 3879.
19. Makarova EA, Korolyova GV and Luk'yanets EA; Edinburgh, England, Sept. 21-23, 1998.
20. Makarova EA, Korolyova GV, Tok OL and Lukyanets EA. *J. Porphyrins Phthalocyanines* 2000; **4**: 525-531.
21. Miwa H, Makarova EA, Ishii K, Luk'yanets EA and Kobayashi N. *Chem. Eur. J*. 2002; **8**: 1082-1090.
22. Nakatsuji H and Hirao K. *J. Chem. Phys*. 1978; **68**: 2053.
23. Nakatsuji H. *Chem. Phys. Lett*. 1978; **59**: 362.
24. Nakatsuji H. *Chem. Phys. Letters* 1979; **67**: 329.
25. Nakatsuji H. *Chem. Phys. Letters* 1979; **67**: 334.
26. Nakatsuji H. In *Computational Chemistry - Reviews of Current Trends* Vol. 2, Leszczynski J. (Ed.) World Scientific: Singapore, 1997; pp 62-124.
27. Monkhorst H. *Int. J. Quantum. Chem. Sympos* 1977; **11**: 421.
28. Dalgaard E and Monkhorst H. *Phys. Rev. A28* 1983; **1217**: 1983.
29. Mukherjee D and Mukherjee PK. *Chem. Phys*. 1979; **39**: 325.
30. Koch H and Joergensen P. *J. Chem. Phys*. 1990; **93**: 3333.
31. Koch H, Jensen HJA, Helgaker T and Joergensen P. *J. Chem. Phys*. 1990; **93**: 3345.
32. Geertsen J, Rittby M and Bartlett RJ. *Chem. Phys. Letters* 1989; **164**: 57.
33. Stanton JF and Bartlett RJ. *J. Chem. Phys*. 1993; **98**: 7029.
34. Ehara M, Ishida M, Toyota K and Nakatsuji H. In *Reviews in Modern Quantum Chemistry*, Sen KD. (Ed.) World Scientific: Singapore, 2002; pp 293-319.
35. Nakatsuji H, Hasegawa J and Hada M. *J. Chem. Phys*. 1996; **104**: 2321.
36. Hohenberg P and Kohn W. *Phys. Rev.* 1964; **136**: B864.
37. Kohn W and Sham LJ. *Phys. Rev.* 1965; **140**: A1133.
38. Parr RG and Yang W. *Density-Functional Theory of Atoms and Molecules*; Oxford Univ. Press: Oxford, 1989
39. Lee C, Yang W and Parr RG. *Phys Rev B* 1988; **37**: 785.
40. Becke AD. *J. Chem. Phys*. 1993; **98**: 5648.
41. Hehre WJ, Ditchfield R and Pople JA. *J. Chem. Phys*. 1972; **56**: 2257.
42. Hariharan PC and Pople JA. *Theor. Chim. Acta* 1973; **28**: 213.
43. Ditchfield R, Hehre WJ and Pople JA. *J. Chem. Phys*. 1971; **54**: 724.
44. Huzinaga S, Andzelm J, Krovkowski M, Radzio-Andzelm E, Sakai Y and Tatewaki H. *Gaussian basis set for molecular calculation*; Elsevier: New York, 1984
45. Huzinaga S. *J. Chem. Phys*. 1965; **42**: 1293.
46. Tokita Y, Hasegawa J and Nakatsuji H. *J. Phys. Chem. A* 1998; **102**: 1843-1849.
47. Nakatsuji H. *Chem. Phys*. 1983; **75**: 425.
48. Frisch MJ, Trucks GW, Schlegel HB, Scuseria GE, Robb MA, Cheeseman JR, J. A. Montgomery J, Vreven T, Kudin KN, Burant JC, Millam JM, Iyengar SS, Tomasi J, Barone V, Mennucci B, Cossi M, Scalmani G, Rega N, Petersson GA, Nakatsuji H, Hada M, Ehara M, Toyota K, Fukuda R, Hasegawa J, Ishida M, Nakajima T, Honda Y, Kitao O, Nakai H, Klene M, Li X, Knox JE, Hratchian HP, Cross JB, Adamo C, Jaramillo J, Gomperts R, Stratmann RE, Yazyev O, Austin AJ, Cammi R, Pomelli C, Ochterski JW, Ayala PY, Morokuma K, Voth GA, Salvador P, Dannenberg JJ, Zakrzewski VG, Dapprich S, Daniels AD, Strain MC, Farkas O, Malick DK, Rabuck AD, Raghavachari K, Foresman JB, Ortiz JV, Cui Q, Baboul AG, Clifford S, Cioslowski J, Stefanov BB, Liu G, Liashenko A, Piskorz P, Komaromi I, Martin RL, Fox DJ, Keith T, Al-Laham MA, Peng CY, Nanayakkara A, Challacombe M, Gill PMW, Johnson B, Chen W, Wong MW, Gonzalez C and Pople JA; Gaussian, Inc.: Pittsburgh PA, 2003.
49. Neya S. Private communication.
50. Edwards L, Dolphin DH, Gouterman M and Adler AD. *J. Mol. Spectrosc*. 1971; **38**: 16.
51. Nagashima U, Takada T and Ohno K. *J. Chem. Phys*. 1986; **85**: 4524.
52. Scheer H and Inhoffen H. In *The Porphyrins*, Vol. II, Dolphin D. (Ed.) Academic press: New York, 1978; pp 45-90.